Great Lakes Spatially Distributed Watershed Model of Water and Materials Runoff

Thomas E. Croley II
Research Hydrologist
Great Lakes Environmental Research Laboratory
2205 Commonwealth Blvd.
Ann Arbor, Michigan 48105-2945
734 741 2238 (office) 734 741 2055 (fax)
Tom.Croley@noaa.gov

Chansheng He
Professor of Geography
Department of Geography
Western Michigan University
3234 Wood Hall
Kalamazoo, Michigan 49008-5424
616 387-3425 (office) 616 387-3442 (fax)
He@wmich.edu

Abstract. Prediction of various ecological system variables or consequences (such as beach closings), as well as effective management of pollution at the watershed scale, require estimation of both point and non-point source material transport through a watershed by hydrological processes. The Great Lakes Environmental Research Laboratory and Western Michigan University are developing an integrated, spatially distributed, physically-based water quality model to evaluate both agricultural non-point source loadings from soil erosion, animal manure, and pesticides, and point source loadings at the watershed level. We are augmenting an existing physically based integrated surface/subsurface hydrology model. It is a two-dimensional, spatially-distributed accounting of moisture in several layers (zones) for every "cell" (1 square kilometer) of a watershed. We modified the model to allow flow routing between adjacent cells surface zones, upper soil zones, lower soil zones, and groundwater zones. We are expanding it, by adding material transport capabilities to it, to include movement of other materials besides water. We will gather information on pollutants in Saginaw Bay watersheds and apply the model to simulate the movement of various materials into the bay, producing estimates useful to ecological system forecasters.

INTRODUCTION

Agricultural non-point source contamination of water resources by pesticides, fertilizers, animal wastes, and soil erosion is a major problem in much of the Great Lakes Basin. Point source contaminations, such as Combined Sewerage Overflows (CSOs), also add wastes to water flows. Soil erosion and sedimentation reduce soil fertility and agricultural productivity, decrease the service life of reservoirs and lakes, and increase flooding and costs for dredging harbors and treating waste-water. Improper management of fertilizers, pesticides, and animal and human wastes can cause increased levels of nitrogen, phosphorus, and toxic substances in both surface water and groundwater. Sediment, waste, pesticide, and nutrient loadings to surface and subsurface waters can result in oxygen depletion and eutrophication in receiving lakes, as well as secondary impacts such as harmful algal blooms and beach closings due to viral and bacterial and/or toxin delivery to affected sites. The U.S. Environmental Protection Agency (EPA) has identified contaminated sediments, urban runoff and storm sewers, and agriculture as the primary sources of pollutants causing impairment of Great Lakes shoreline waters (USEPA 2002). Prediction of various ecological system variables or consequences (such as beach closings), as well as effective management of pollution at the watershed scale, require estimation of both point and non-point source material transport through a watershed by hydrological processes. However, currently there are no integrated spatially distributed physically based watershed-scale hydrological/water quality models available to evaluate

movement of materials (sediments, animal and human wastes, agricultural chemicals, nutrients, etc.) in both surface and subsurface waters in the Great Lakes watersheds.

The Great Lakes Environmental Research Laboratory (GLERL) and Western Michigan University are developing an integrated, spatially distributed, physically-based water quality model to evaluate both agricultural non-point source loading from soil erosion, fertilizers, animal manure, and pesticides, and point source loadings at the watershed level. GLERL is augmenting an existing physically based distributed surface/subsurface hydrology model (their Distributed Large Basin Runoff Model) by adding material transport capabilities to it. This will facilitate effective Great Lakes watershed management decision-making, by allowing identification of critical risk areas and tracking different sources of pollutants for implementation of water quality programs, and will augment ecological prediction efforts. This paper briefly reviews distributed watershed models of water and agricultural materials runoff and identifies their limitations and then presents our resultant distributed model of water and material movement within a watershed and indicates anticipated improvements. A companion paper discusses the application of this model to water quality issues in the Saginaw Bay watersheds in Michigan.

DISTRIBUTED AGRICULTURAL RUNOFF MODELS

Estimating point and non-point source pollutions and CSOs is critical to planning and enforcement agencies in protection of surface water and groundwater quality. During the past four decades, a number of simulation models have been developed to aid in the understanding and management of surface runoff, sediment, nutrient leaching, and pollutant transport processes. The widely used water quality models include ANSWERS (Areal Non-point Source Watershed Environment Simulation) (Beasley and Huggins 1980), CREAMS (Chemicals, Runoff and Erosion from Agricultural Management Systems) (Knisel 1980), GLEAMS (Groundwater Loading Effects of Agricultural Management Systems) (Leonard et al. 1987), AGNPS (Agricultural Non-point Source Pollution Model (Young et al. 1989), EPIC (Erosion Productivity Impact Calculator) (Sharpley and Williams 1990), and Soil and Water Assessment Tool (SWAT) (Arnold et al. 1998) to name a few. These models all use the SCS Curve Number method, an empirical formula for predicting runoff from daily rainfall. Although the Curve Number method has been widely used worldwide, researchers have expressed concern that it does not reproduce measured runoff from specific storm rainfall events because the time distribution is not considered (Kawkins 1978; Wischmeier and Smith 1978; Beven 2000; Garen and Moore 2005). Limitations of the Curve Number method also include 1) no explicit account of the effect of the antecedent moisture conditions in runoff computation, 2) difficulties in separating storm runoff from the total discharge hydrograph, and 3) runoff processes not considered by the empirical formula (Beven 2000; Garen and Moore 2005). Consequently, estimates of runoff and infiltration derived from the Curve Number method may not well represent the actual. As sediment, nutrient, and pesticide loadings are directly related to infiltration and runoff, use of the Curve Number method may also result in incorrect estimates of non-point source pollution rates.

Considering the limitations of the Curve Number method, ANSWERS, CREAMS, GLEAMS, AGNPS, and SWAT were developed to assess impacts of different agricultural management practices, not to predict exact pesticide, nutrient, and sediment loading in a study area (Ghadiri and Rose 1992; Beven 2000; Garen and Moore 2005). In addition, most water quality models, such as CREAMS and GLEAMS, are field-size models and cannot be used directly at the watershed scale. Applications of these models have been limited to field scale or small experimental watersheds. Some models, e.g. ANSWERS, CREAMS, EPIC, and AGNPS, also do not consider subsurface and groundwater processes.

Recently, several water quality models have been modified to take into consideration available multiple physical and agricultural databases. The US EPA designated two of the most widely used water quality models, SWAT and HSPF (Hydrologic Simulation Program in FORTRAN) (Bicknell et al. 1996), for simulation of hydrology and water quality nationwide. SWAT is a comprehensive watershed model and considers runoff production, percolation, evapotranspiration, snowmelt, channel and reservoir routing, lateral subsurface flow, groundwater flow, sediment yield, crop growth, nitrogen and phosphorous, and pesticides. But it uses the Curve Number method for estimating runoff and therefore has those same

limitations the Curve Number method has in runoff simulation. The basic simulation unit in SWAT is the sub-watershed, instead of a grid network, thus limiting its incorporation of spatial variability in simulating hydrologic processes.

Evolved from the Stanford Watershed Model (Crawford and Linsey 1966), HSPF is one of the most extensively used general hydrologic and water quality models (Bicknell et al. 1996). Under the auspices of the US EPA, the first version of the HSPF was completed in 1980. Since then, the model has gone through extensive revisions, corrections, refinements, and validations in many areas and is one of the three simulation models included in BASINS (Better Assessment Science Integrating Point and Non-point Sources), the US EPA's watershed modeling tools for support of water quality management programs throughout the country (Lahlou et al. 1998). HSPF utilizes time series meteorology data to simulate hydrological processes in both pervious and impervious land segments. The hydrological processes in the model include accumulation and melting of snow and ice, water budget, sediment transport, soil moisture and temperature. The water quality modules of the model include concentration and transport of nitrogen, phosphorus, pesticides, and other pollutants. However, HSPF requires extensive input parameters such as wind speed, dew point temperature, potential evapotranspiration, and channel characteristics. Many of these parameters are not available in most watersheds, particularly large watersheds. In addition, HSPF is basically a lumped parameter model and thus lacks consideration of spatial variability of hydrological processes. Moreover, neither SWAT nor HSPF considers non-point sources from animal manure and CSOs and infectious diseases. Thus, there is an urgent need for the development of a spatially distributed physically-based watershed model that simulates both point and non-point source pollutions in the Great Lakes Basin.

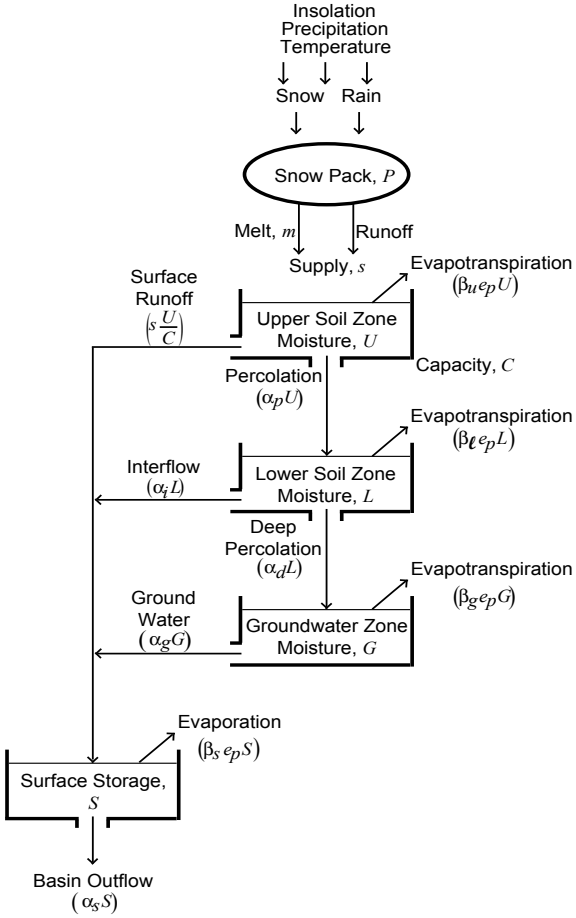

Figure 1. LBRM Tank Cascade Schematic.

LARGE BASIN RUNOFF MODEL

GLERL developed a large-scale operational model in the 1980s for estimating rainfall/runoff relationships on the 121 large watersheds surrounding the Laurentian Great Lakes. It is physically based to provide good representations of hydrologic processes and to ensure that results are tractable and explainable. It is a lumped-parameter model of basin outflow consisting of a cascade of moisture storages or "tanks" each modeled as a linear reservoir, where tank outflows are proportional to tank storage. The mass balance schematic is shown in Figure 1. Daily precipitation, temperature, and insolation (the latter available from meteorological summaries as a function of location) may be used to determine snow pack accumulations, snow melt (degree-day computations), and net supply, s. The net supply is divided into surface runoff, $s\frac{U}{C}$, and infiltration to the upper soil zone, $s - s\frac{U}{C}$, in relation to the upper soil zone moisture content, U, and the fraction it represents of the upper soil zone capacity, C (variable area infiltration). Percolation to the lower soil zone, $\alpha_p U$, and evapotranspiration, $\beta_u e_p U$, are taken as outflows from a

linear reservoir (flow is proportional to storage). Likewise, interflow from the lower soil zone to the surface, $\alpha_i L$, evapotranspiration, $\beta_\ell e_p L$, and deep percolation to the groundwater zone, $\alpha_d L$, are linearly proportional to the lower soil zone moisture content, L. Groundwater flow, $\alpha_g G$, and evapotranspiration from the groundwater zone, $\beta_g e_p G$, are linearly proportional to the groundwater zone moisture content, G. Finally, basin outflow, $\alpha_s S$, and evaporation from the surface storage, $\beta_s e_p S$, depend on its content, S. Additionally, evaporation and evapotranspiration are dependent on potential evapotranspiration, e_p, as determined by joint consideration of the available moisture and the heat balance over the watershed. Total heat available during the day is estimated from air temperature and split between potential and actual evapotranspiration. Actual evaporation is taken proportional to both the potential and to storage. Thus actual and potential evapotranspiration are complementary. The "alpha" coefficients (α) represent linear reservoir proportionality factors and the "beta" coefficients (β) represent partial linear reservoir coefficients associated with evapotranspiration.

Mass conservation equations (Croley 2002) are repeated here for convenience as differential equations with respect to time t.

$$\frac{d}{dt}U = s\left(1-\frac{U}{C}\right) - \alpha_p U - \beta_u e_p U \tag{1}$$

$$\frac{d}{dt}L = \alpha_p U - \alpha_i L - \alpha_d L - \beta_\ell e_p L \tag{2}$$

$$\frac{d}{dt}G = \alpha_d L - \alpha_g G - \beta_g e_p G \tag{3}$$

$$\frac{d}{dt}S = s\frac{U}{C} + \alpha_i L + \alpha_g G - \alpha_s S - \beta_s e_p S \tag{4}$$

Equations (1)—(4) can be expressed in the general form:

$$dZ + (\Sigma\alpha) Z dt = f(t) dt \tag{5}$$

where Z = storage, $(\Sigma\alpha)$ = sum of linear reservoir constants for all outflows, and $f(t)$ = sum of time-dependent inflows. Standard procedures (Rainville 1964) yield:

$$Z_t = e^{-(\Sigma\alpha)t}\left[Z_0 + \int_0^t f(u) e^{(\Sigma\alpha)u} du\right] \tag{6}$$

where the subscript is time. In solving (1)—(4) for some time increment $(0,t)$, we generally take net supply and potential evapotranspiration as uniform over the increment. Storage values at the end of a time increment are computed from values at the beginning. In the analytical solution, results from one storage zone are used in other zones where their outputs appear as inputs. There are several different solutions, depending upon the relative magnitudes of all coefficients in (1)—(4). Croley (2002) solved the equations, yielding storages at the end of a time increment (U_t, L_t, G_t, and S_t) as functions of the inputs, parameters, and beginning-of-time-increment storages (storages at the end of the previous time increment: U_0, L_0, G_0, and S_0). Since the variables s and e_p change from one time increment to another, then the appropriate analytical result, as well as its solution, varies with time. Mathematical continuity between solutions is preserved however. These results are summarized elsewhere (Croley 2002). The model is physically based and is calibrated by finding its nine parameter values by systematically searching the parameter space. We use gradient search techniques to minimize the root mean square error (RMSE) between modeled basin outflow and actual.

The large basin runoff model is used and has been used for the daily time interval at GLERL for a variety of studies, including hydrological forecasting in GLERL's Advanced Hydrologic Prediction System, which gives probabilistic outlooks of Great Lakes evaporation, runoff, and lake levels, among others.

Uses also include 5 past studies of climate change impacts on Great Lakes hydrology, and several analyses of management and regulation scenarios.

DISTRIBUTED WATERSHED MODEL

The Large Basin Runoff Model is used here in application to individual sub areas (cells) within a watershed by modifying its structure to accept upstream flows. We converted it to a two-dimensional, spatially-distributed accounting of moisture in several layers (zones) for every 1 sq. km. cell of a watershed. We first modified it to compute potential and actual evapotranspiration as if the two are independent, appropriate for small areas. We then modified it to allow lateral flows between all storage zones (tanks) in adjacent cells. This involved modifying model code to direct one cell's storage's lateral outflow into another cell's storage zone as inflow. We allowed lateral flows between cells for all moisture storages: upper soil zones, lower soil zones, groundwater zones, and surface zones. From Figure 2,

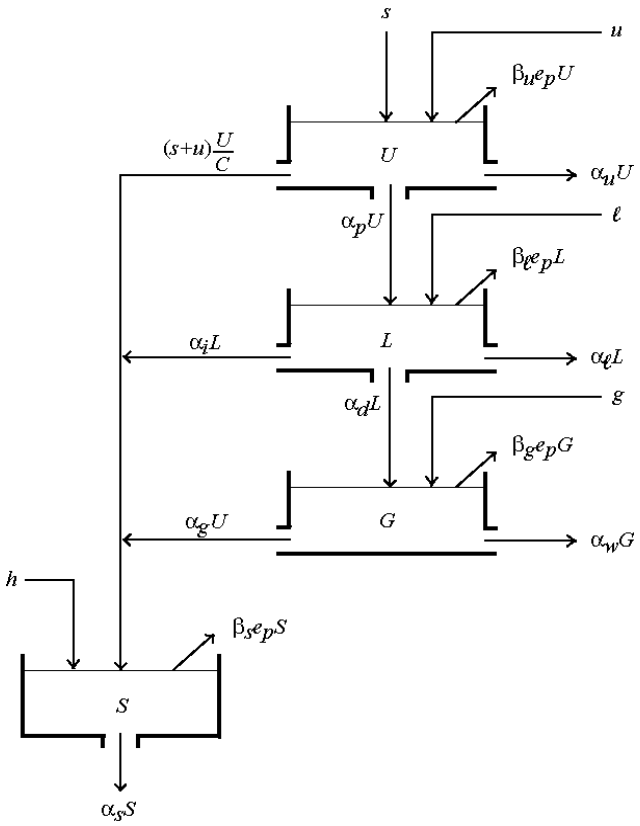

Figure 2. Distributed LBRM Tank Cascade Schematic for a Single Cell.

$$\frac{d}{dt}U = s + u - (s+u)\frac{U}{C} - \alpha_p U - \alpha_u U - \beta_u e_p U \quad (7)$$

$$\frac{d}{dt}L = \alpha_p U - \alpha_i L - \alpha_d L - \alpha_\ell L + \ell - \beta_\ell e_p L \quad (8)$$

$$\frac{d}{dt}G = \alpha_d L - \alpha_g G - \alpha_w G + g - \beta_g e_p G \quad (9)$$

$$\frac{d}{dt}S = (s+u)\frac{U}{C} + \alpha_i L + \alpha_g G - \alpha_s S + h - \beta_s e_p S \quad (10)$$

where u = lateral flow rate from upstream upper soil zone, α_u = linear reservoir coefficient for lateral flow to downstream upper soil zone, ℓ = lateral flow rate from upstream lower soil zone, α_ℓ = linear reservoir coefficient for lateral flow to downstream lower soil zone, g = lateral flow rate from upstream groundwater zone, α_w = linear reservoir coefficient for lateral flow to downstream groundwater zone, h = lateral flow rate from upstream surface zone, and α_s now becomes the linear reservoir coefficient for lateral flow to a downstream surface zone. We derived corrector equations (Croley and He 2005b) to express (7)—(10) in terms of (1)—(4) and changed the computer code correspondingly.

We have discretized 18 watersheds to date. The elevation map for the Kalamazoo River watershed, in southwestern Michigan is shown in Figure 3. We started with elevations taken from a 1 km digital elevation model (DEM) available from the United States Geological Survey. We soon adopted their 30m DEM to derive 1km elevations and slopes as their 1 km DEM proved insufficient. Additionally, we compiled databases of all soil, land use, and derived parameters and all daily meteorology for each square kilometer of each watershed.

Each cell's inflow hydrographs must be known before its outflow hydrograph can be modeled; therefore we arranged calculations by flow network to assure this. The flow network is implemented to minimize the number of pending hydrographs in computer storage and the time required for them to be in computer storage. We added flow routing for all upstream to downstream cell flows and used the same

network for surface, upper soil, lower soil, and groundwater storages. A small example flow routing derived from an elevation map is shown in Figure 4. We implemented routing network computations as a recursive routine to compute outflow that calls itself to compute inflows (which are upstream outflows) (Croley and He 2005a,b). In application, we use the same gradient search technique to minimize RMSE between modeled and actual basin outflow by selecting the best spatial averages for each parameter; the spatial variation of each parameter was allowed to vary as a selected watershed characteristic, as shown here.

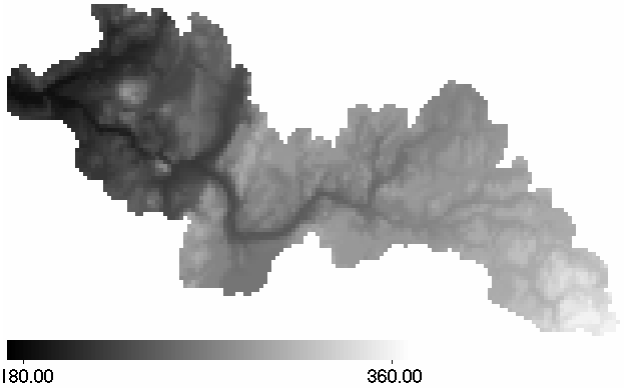

Figure 3. Kalamazoo Watershed Elevations (m).

$$\left(\alpha_p\right)_i = \bar{\alpha}_p \; f(K_i^U, 80\%) \tag{11}$$

$$\left(\beta_u\right)_i = \bar{\beta}_u \; f(K_i^U, 80\%) \tag{12}$$

$$\left(\alpha_i\right)_i = \bar{\alpha}_i \; f(K_i^L, 80\%) \tag{13}$$

$$\left(\alpha_d\right)_i = \bar{\alpha}_d \; f(K_i^L, 80\%) \tag{14}$$

$$\left(\beta_\ell\right)_i = \bar{\beta}_\ell \; f(K_i^L, 80\%) \tag{15}$$

$$\left(\alpha_g\right)_i = \bar{\alpha}_g \; f(K_i^L, 80\%) \tag{16}$$

$$\left(\alpha_s\right)_i = \bar{\alpha}_s \; f(\frac{\sqrt{s_i}}{\eta_i}, 80\%) \tag{17}$$

$$\left(\alpha_u\right)_i = \bar{\alpha}_u \; f(K_i^U, 80\%) \tag{18}$$

$$\left(\alpha_\ell\right)_i = \bar{\alpha}_\ell \; f(K_i^L, 80\%) \tag{19}$$

$$\left(\alpha_w\right)_i = \bar{\alpha}_w \; f(K_i^L, 80\%) \tag{20}$$

$$\left(C\right)_i = \bar{C} \; f(C_i^U, 80\%) \tag{21}$$

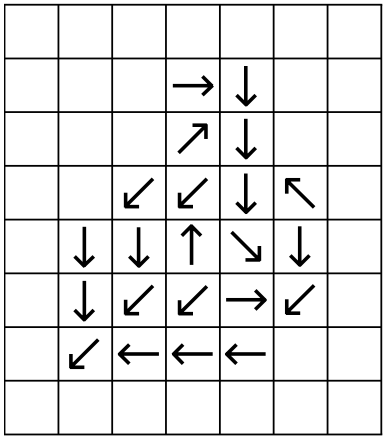
Figure 4. Watershed grid flows.

$$f(x_i, \varepsilon) = \left(\frac{x_i}{\frac{1}{n}\sum_{j=1}^{n} x_j} - 1 \right) \frac{\varepsilon}{100\%} + 1 \tag{22}$$

where $\left(\alpha_\bullet\right)_i$ = linear reservoir coefficient for cell i, $\bar{\alpha}_\bullet$ = spatial average value of linear reservoir coefficient (from parameter calibration), $\left(\beta_\bullet\right)_i$ and $\bar{\beta}_\bullet$ are defined similarly for partial linear reservoir coefficients (used in evapotranspiration), $\left(C\right)_i$ and $\bar{C}$ are defined similarly for the upper soil zone capacity, K_i^U = upper and K_i^L = lower soil zone permeability in cell i, s_i = slope of cell i, η_i = Manning's roughness coefficient for cell i, C_i^U = upper soil zone available water capacity, x_i = data value for cell i, and n = number of cells in the watershed.

To speed up calibrations, we preprocess all meteorology for all watershed cells and preload it into computer memory. We used the model to look at modeling alternatives, including alternative evapotranspiration calculations, spatial parameter patterns, and solar insolation estimates. We also explored scaling effects in using lumped parameter model calibrations to calculate initial distributed model parameter values (Croley and He 2005a; Croley et al. 2005).

MATERIALS RUNOFF MODEL

Consider now the addition of some material or pollutant dissolved in, or carried by, the water flows in Figure 2, except that none is considered to be evaporated; see Figure 5. At any time, let the concentration of this conservative pollutant in the inflow u be c_u and in the supply s be c_s. If these flows do not mix together, then the fraction $\frac{U}{C}$ of each of these flows runs off directly (without even entering the upper soil zone) and the surface runoff of pollutant is $\left(sc_s + uc_u\right)\frac{U}{C}$. If the concentration in the upper soil zone moisture storage U is c_U, then the percolating pollutant is $\alpha_p U c_U$ and the lateral pollutant flow downstream to the next cell's upper soil zone is $\alpha_u U c_U$. Taking pollutant movement with evaporation as zero, mass continuity (of the pollutant) gives:

$$\frac{d}{dt}\left(Uc_U\right) = sc_s + uc_u - \left(sc_s + uc_u\right)\frac{U}{C} - \alpha_p U c_U - \alpha_u U c_U \tag{23}$$

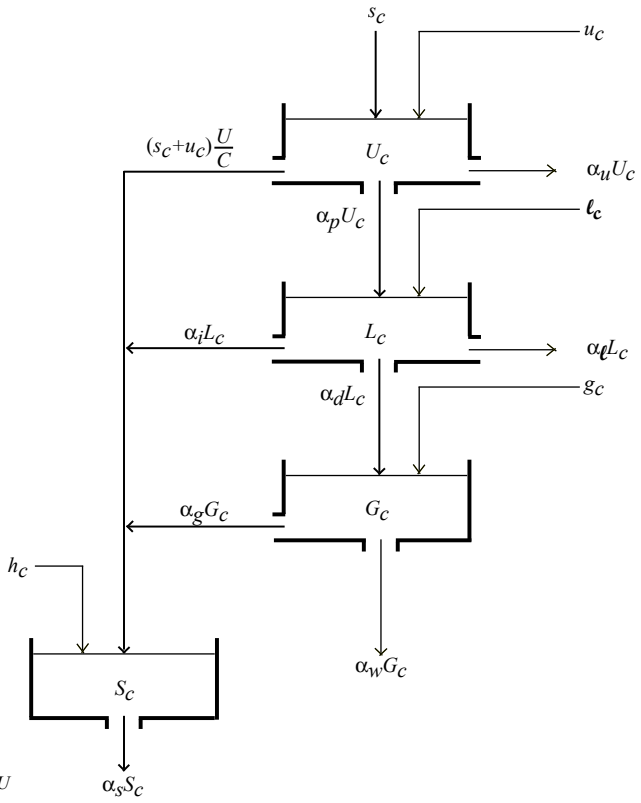

Figure 5. Distributed "Pollutant" Flows Model Schematic for a Single Cell.

or

$$\frac{d}{dt}U_c = s_c + u_c - \left(s_c + u_c\right)\frac{U}{C} - \alpha_p U_c - \alpha_u U_c \tag{24}$$

where $s_c = sc_s$, $u_c = uc_u$, and $U_c = Uc_U$.

Likewise from Figure 5, mass continuity of the pollutant gives:

$$\frac{d}{dt}L_c = \alpha_p U_c - \alpha_i L_c - \alpha_d L_c - \alpha_\ell L_c + \ell_c \tag{25}$$

$$\frac{d}{dt}G_c = \alpha_d L_c - \alpha_g G_c - \alpha_w G_c + g_c \tag{26}$$

$$\frac{d}{dt}S_c = \left(s_c + u_c\right)\frac{U}{C} + \alpha_i L_c + \alpha_g G_c - \alpha_s S_c + h_c \tag{27}$$

where L_c, G_c, and S_c are the amounts of pollutant in the lower soil zone, the groundwater zone, and surface storage, respectively, and ℓ_c, g_c, and h_c are the upstream pollutant flows from the lower soil zone, the groundwater zone, and surface storage, respectively.

Solution

As previously mentioned, Croley (2002) solved (1)—(4) simultaneously, deriving 30 analytical solutions, and Croley and He (2005b) derived corrector equations to the analytical solutions. However, consideration of an analytical solution of (7)—(10) and (24)—(27) reveals even more multiple solutions; while tractable, a simpler approach is desired. The approach taken here is to use a numerical solution based on finite difference approximations of (7)—(10) and (24)—(27). Consider (7) approximated with finite differences,

$$\Delta U \simeq (s+u)\Delta t - \left(\frac{(s+u)}{C} + \alpha_p + \alpha_u + \beta_u e_p \right) \bar{U} \Delta t \tag{28}$$

where ΔU = change in upper soil zone moisture storage over time interval Δt and $\bar{U}$ = average upper soil zone moisture storage over time interval Δt. By taking $\Delta U = U - U_0$ (where U_0 and U are beginning-of- and end-of-time-interval storages, respectively) and $\bar{U} \simeq U$, (28) becomes

$$U \simeq \frac{U_0 + (s+u)\Delta t}{1 + \left(\frac{s+u}{C} + \alpha_p + \alpha_u + \beta_u e_p \right) \Delta t} \tag{29}$$

Equation (29) is good for small Δt and as $\Delta t \to 0$, (29) approaches the true solution (converges) to (7). Likewise, using similarly defined terms, (8)—(10) become

$$L \simeq \frac{L_0 + (\alpha_p U + \ell)\Delta t}{1 + (\alpha_i + \alpha_d + \alpha_\ell + \beta_\ell e_p)\Delta t} \tag{30}$$

$$G \simeq \frac{G_0 + (\alpha_d L + g)\Delta t}{1 + (\alpha_g + \alpha_w + \beta_g e_p)\Delta t} \tag{31}$$

$$S \simeq \frac{S_0 + \left(\frac{s+u}{C} U + \alpha_i L + \alpha_g G + h \right) \Delta t}{1 + (\alpha_s + \beta_s e_p)\Delta t} \tag{32}$$

Similarly, the numerical solution for (24)—(27) becomes

$$U_c \simeq \frac{U_{c0} + (s_c + u_c)\Delta t - (s_c + u_c)\frac{U}{C}\Delta t}{1 + (\alpha_p + \alpha_u)\Delta t} \tag{33}$$

$$L_c \simeq \frac{L_{c0} + (\alpha_p U_c + \ell_c)\Delta t}{1 + (\alpha_i + \alpha_d + \alpha_\ell)\Delta t} \tag{34}$$

$$G_c \simeq \frac{G_{c0} + (\alpha_d L_c + g_c)\Delta t}{1 + (\alpha_g + \alpha_w)\Delta t} \tag{35}$$

$$S_c \simeq \frac{S_{c0} + \left(\frac{s_c + u_c}{C} U + \alpha_i L_c + \alpha_g G_c + h_c \right) \Delta t}{1 + \alpha_s \Delta t} \tag{36}$$

where terms are defined for material flows similarly as they are defined for water flows.

Initial and boundary conditions

Suppose that at time $t = 0$, there exists a pollutant deposit on top of the upper soil zone of P_0. Precipitation or snowmelt on top of this deposit will produce a supply s to the upper soil zone that will dissolve some of this pollutant, producing a pollutant concentration c_s. If we regard this process as independent of other flows to the top of the upper soil zone (u and $u_c = uc_u$), we can model the pollutant uptake as follows.

$$\begin{aligned} c_s &= c_m \qquad \text{if } sc_m\Delta t \le P_0 \\ &= \frac{P_0}{s\Delta t} \qquad \text{if } sc_m\Delta t > P_0 \end{aligned} \tag{37}$$

$$P = P_0 - sc_s\Delta t \tag{38}$$

where c_m = maximum concentration physically permitted by contact between water and pollutant and P = pollutant deposit at the end of time interval Δt. Then the pollutant delivered to the top of the upper soil zone would be $s_c + u_c = sc_s + uc_u$ as used in (23), (24), (27), (33), and (36).

Alternatively, we may presume that s_c and u_c mix before runoff and infiltration occur; when they are mixed, they both have concentration c_s and we can model the pollutant uptake as follows (taking c_u = lateral flow rate pollutant concentration of the upstream upper soil zone before mixing).

$$\begin{aligned} c_s &= c_m && \text{if } sc_m\Delta t + u\left(c_m - c_u\right)\Delta t \le P_0 \\ &= \frac{P_0 + uc_u\Delta t}{\left(s+u\right)\Delta t} && \text{if } sc_m\Delta t + u\left(c_m - c_u\right)\Delta t > P_0 \end{aligned} \tag{39}$$

$$P = P_0 - sc_s\Delta t - u\left(c_s - c_u\right)\Delta t \tag{40}$$

The pollutant delivered to the top of the upper soil zone in this case would be $s_c + u_c = \left(s+u\right)c_s$ and $u_c = uc_s$ would be used in place of $u_c = uc_u$ in (23), (24), (27), (33), and (36).

As (29)—(36) and either (37)—(38) or (39)—(40) are used over time interval Δt, end-of-time-interval values are computed from beginning-of-time-interval values (e.g., U from U_0 and P from P_0). These end-of-time-interval values for one time interval become beginning-of-time-interval values for the subsequent time interval.

Testing

As a test of (29)—(32), we used them for Δt = 1.5 minutes to approximate the solution of (7)—(10) over about 17 years of daily values for the Maumee River watershed (Croley and He 2005b) and found them identical (in all variables) through three significant digits (all that were inspected) with the exact analytical solution. For Δt = 15 minutes, the solution was nearly identical with only an occasional difference of one in the third significant digit. As the Maumee River watershed has a very "flashy" response to precipitation (very fast upper soil and surface storage zones) these comparisons are deemed significant and the time intervals should be more than adequate for the slower response of lower soil and groundwater zones (the Maumee application has no lower soil or groundwater zones).

EXAMPLE APPLICATION

Selected lateral flows simulated by the model for the upper soil zone, ground water zone, and surface zone are shown in Figure 6 for the Kalamazoo River watershed for the first two months of 1952. Although the simulation was daily, the flows are shown weekly in Figure 6. The initial conditions for this simulation included 1 cm of (arbitrary) pollutant on the surface of the watershed on January 1, 1952. Within two weeks it was gone from the surface (@ c_m = 1.0 cm/d). Columns 1—3 in Figure 6 show that lateral water flows in the watershed were fairly uniform for the period with perhaps higher surface water flows on January 1 and 15 (more of the streamflow network is seen to respond then). Column 4 illustrates that even at the end of day 1, the upper soil zone already had pollutant in it; USZ pollutant flows peak on January 15 and slowly taper off through the end of February. Pollutant did not appear in any sizable manner in the groundwater zone until the end of February, as illustrated in column 5 of Figure 6. The pollutant flow in the surface network, shown in the last column in Figure 6, responds midway between the USZ and GWZ responses. There is a high flush on the first day, corresponding with the initial condition (placing pollutant on the surface of the watershed at the beginning of day 1) and the increased surface water flow; the surface pollutant map shows extensive response. The surface response then drops off as pollutant is only available in the USZ and GWZ. However, on January 15, the surface pollutant response increases with the flush of water through the USZ that occurs then (see third row in columns 3 and 4 in Figure 6).

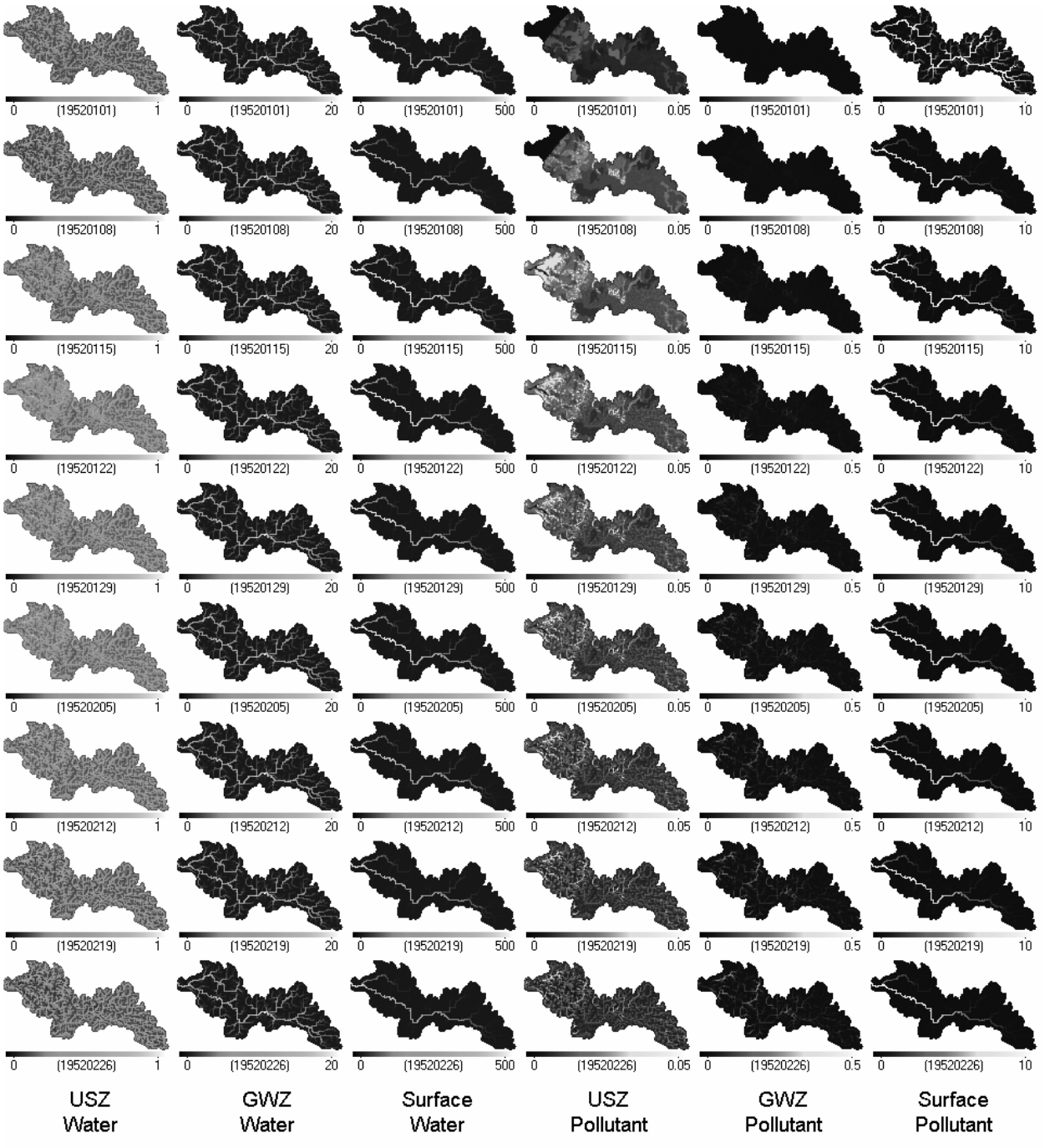

Figure 6. Kalamazoo Model Lateral Flows (cm/d).

NEXT STEPS

We are about to develop an hourly version of the model from the present daily version, for better tracking of the movement of water and materials within a watershed. We plan to change the model code structure to include diurnal hydrology concepts and to provide for the massive data handling necessary for hourly meteorology (precipitation and minimum and maximum air temperature over every square kilometer of a watershed's surface). We are building hourly model data streams in cooperation with the National Severe Storms Laboratory to be operated in near real time; we are planning on preprocessing the data to aid in

the repetitive simulations employed in calibration. (We will also incorporate these data streams into existing daily models as well as into the altered hourly model structure. We hope to demonstrate improved water accounting and accurate water level forecasting in GLERL's Advanced Hydrologic Prediction System with the improved daily models.) These hourly data streams will directly couple high resolution, multiple sensor quantitative precipitation estimates to the hydrologic models. We will also expand the data streams in the near future to use both Canadian and US weather observational systems. (NOAA's National Severe Storms Laboratory is currently using Canadian radar data and testing its suitability.)

We will add sedimentation and selected non-point source pollutant transport to the hourly model, by using the Modified Universal Soil Loss Equation and relevant erosion and pollutant loadings. (Hence, we will treat transport as sufficient to always carry the erosion loss and not consider deposition.) We are surveying the Saginaw Bay watersheds to gather information on pollutants and their sources and to build databases for use in model applications. These include information on animal manure, pesticides, and fertilizer to estimate nitrogen, phosphorus, and other pollutant loadings. It is not presently clear how necessary or available this information will be in near real time. Finally, we will make application to the Saginaw Bay watersheds; we hope to simulate the movement of various materials into the bay, producing estimates useful to ecological system forecasters.

SUMMARY

Prediction and management of watershed water quality require estimation of non-point source material movement throughout the watershed. We briefly review distributed agricultural runoff models to learn that there are no integrated spatially distributed physically based watershed-scale hydrological/water quality models available to evaluate movement of materials in both surface and subsurface waters. Either the hydrology is limited to very simple empirical descriptions or the application is made to only very coarse spatial discretizations of the watershed. We describe an existing lumped-parameter conceptual water balance model of watershed hydrology and adapt it into a spatially distributed model of runoff. It employs moisture storage in the upper and lower soil zones, in a groundwater zone, and on the surface with lateral flows from all storages into adjacent grid cells defined over the watershed. By applying the surface drainage network to all storage lateral flows, we can trace the movement of water throughout the watershed. We further adapt the distributed model to incorporate the storage and movement of an arbitrary material, conservative in nature, and to trace its movement throughout the watershed. By employing a numerical solution instead of the analytical solution used in the water-only model, we are able to easily represent the water balances of both water and an arbitrary conservative pollutant spatially throughout all storage zones in the watershed. Testing reveals that the numerical solution converges quite nicely to the analytical solution for a 1-km^2 grid on a watershed with a very fast response. By assigning initial pollutant surface amounts and introducing a single parameter (the maximum concentration allowable of pollutant in water in a day), we can model the movement of pollutant. In a simple example on the Kalamazoo River watershed, in which a uniform layer of pollutant is assumed initially, we present the consecutive spatial distributions that occur over a two-month simulation, illustrating how the model could be used to model real-world material watershed movement. We outline the next steps in model development necessary to use the model in other real-world situations, including the development of an hourly (instead of daily model), the incorporation of sedimentation (erosion), the incorporation of other specific materials (animal manure, pesticides, fertilizers), and the building of surveyed databases necessary to initialize the model. We plan to apply the model then to the Saginaw Bay watersheds to produce estimates useful to ecological system forecasters in assessing flows into Lake Huron.

ACKNOWLEDGMENTS

We gratefully acknowledge the support of the Key Lab of Poyang Lake Ecological Environment and Resource Development of Jiangxi Normal University. This is GLERL Contribution No. 1358.

REFERENCES

Arnold, G., R. Srinavasan, R.S. Muttiah, and J.R. Williams, 1998. Large area hydrologic modeling and Assessment. Part I. Model Development. *Journal of the American Water Resources Association*, **34**:73-89.

Beasley, D.B. and L.F. Huggins, 1980. ANSWERS (Areal Nonpoint Source Wateshed Environment Simulation) - User's Manual. Department of Agricultural Engineering, Purdue University, West Lafayette, Indiana.

Beven, K. J., 2000. *Rainfall-Runoff Modeling: The Primer*. John Wiley & Sons, Ltd., New York.

Bicknell, B. R., J. C. Imhoff, J. Kittle, A. S. Donigian, and R. C. Johansen, 1996. Hydrological Simulation Program—FORTRAN, User's Manual for Release 11. U. S. Environmental Protection Agency, Environmental Research Laboratory, Athens, Georgia.

Crawford, N. H., and R. K. Linsley, 1966. Digital simulation in hydrology: Stanford Watershed Model IV. Technical Report 39, Dept. of Civil Engineering, Stanford University, California.

Croley, T. E., II, 2002. Large basin runoff model. In *Mathematical Models in Watershed Hydrology* (V. Singh, D. Frevert, and S. Meyer, Eds.), Water Resources Publications, Littleton, Colorado, 717-770.

Croley, T. E., II, and C. He, 2005a. Distributed-parameter large basin runoff model. I: Model development. *Journal of Hydrologic Engineering*, **10**(3):173-181.

Croley, T. E., II, and C. He, 2005b. Watershed Surface and Subsurface Spatial Intraflows. *Journal of Hydrologic Engineering*, (in press).

Croley, T. E., II, C. He, and D. H. Lee, 2005. Distributed-parameter large basin runoff model. II: Application. *Journal of Hydrologic Engineering*, **10**(3):182-191.

Garen, D. C., and D. S. Moore, 2005. Curve Number hydrology in water quality modeling: uses, abuses, and future directions. *Journal of the American Water Resources Association*, **41**(1):377-388.

Ghadiri, H. and C. W. Rose. (ed.) 1992. *Modeling Chemical Transport in Soils: Natural and Applied Contaminants*. Lewis Publishers, Ann Arbor, Michigan.

Kawkins, R.H., 1978. Runoff Curve Number Relationships with Varying Site Moisture. *Journal of the Irrigation and Drainage Division*, **104**:389-398.

Knisel, W.G. (Editor), 1980. CREAMS: A Fieldscale Model for Chemical, Runoff, and Erosion from Agricultural Management Systems. USDA, Science and Education Administration, Conservation Report No. 26, Washington, D.C.

Lahlou, N., L. Shoemaker, S. Choudhury, R. Elmer, A.Hu, H. Manguerra, and A. Parker. 1998. BASINS V.2.0 User's Manual. U.S. Enrionmental Protection Agency Office of Water, EPA-823-B-98-006, Washington, D.C.

Leonard, R.A. W.G. Knisel, and D.A. Still, 1987. GLEAMS: Groundwater Loading Effects of Agricultural Management Systems. *Transactions of ASAE*, **30:**1403-1418.

Rainville, E. D., 1964. *Elementary Differential Equations*. Third Edition, MacMillan, New York, New York, 36—39.

Sharpley, A.N. and J.R. Williams (Editors), 1990. EPIC-Erosion/Productivity Impact Calculator. USDA, Agricultural Research Service, Technical Bulletin No. 1768, Washington, D.C. 235 pp.

U.S. Environmental Protection Agency, 2002. National Water Quality Inventory 2000 Report. EPA-841-R-02-001, Washington DC.

Wischmeier, W.H. and D.D. Smith, 1978. Predicting Rainfall Erosion Losses. Agricultural Handbook No. 537, U.S. Department of Agriculture, Washington, D.C.

Young, R.A., C.A. Onstad, D.D. Bosch, and W.P. Anderson, 1989. AGNPS: A Non-Point-Source Pollution Model for Evaluating Agricultural Watersheds. *Journal of Soil and Water Conservation,* **44**(2):168-173

Proceedings of the International Conference on Poyang Lake Wetland Ecological Environment, Jiangxi Normal University, Nanchang, Jiangxi, P.R. China, June 27, 2005, 12 pp. (2005).